Inorg. Chem. **1994**, *33*, 1614–1621

Synthesis and Characterization of (*o*-Phenylenebis(dimethylarsine))rhenium(III) and -(V) Complexes with Thiolato Ligands[†]

Lihsueh (Sherry) Chang,[1] Mary Jane Heeg,*[,2] and Edward Deutsch*[,1,3]

Biomedical Chemistry Research Center, Department of Chemistry, University of Cincinnati,
Cincinnati, Ohio 45221-0172, and Department of Chemistry, Wayne State University,
Detroit, Michigan 48202-3929

Received April 27, 1993[⊗]

The cationic Re(III) complexes *trans*-$[\mathrm{Re(SCH_2CH_3)_2(DIARS)_2}]^+$ and *cis*- and *trans*-$[\mathrm{Re(SC_6H_5)_2(DIARS)_2}]^+$, where DIARS = *o*-phenylenebis(dimethylarsine), have been synthesized and characterized. Preparation of these complexes proceeds from the Re(V) species $[\mathrm{ReOCl_3(PPh_3)_2}]$ by reaction with excess thiol and diarsine at 100 °C. The complexes have been characterized by FAB mass spectroscopy, visible–UV spectroscopy, elemental analysis, and cyclic voltammetry. X-ray crystal structure analyses of two of these complexes confirm that they have *trans* geometry. *trans*-$[\mathrm{Re(SCH_2CH_3)_2(DIARS)_2}]\mathrm{PF_6}$, chemical formula $\mathrm{ReAs_4S_2PF_6C_{24}H_{42}}$, crystallizes in the orthorhombic space group *Pbcn* with $Z = 4$ and lattice parameters $a = 13.505(2)$ Å, $b = 12.490(5)$ Å, $c = 21.703(4)$ Å, and $V = 3361(2)$ Å^3. Important structural parameters are Re–S = 2.284(3) Å, Re–S–C = 119.5°, and Re–As = 2.480(4) Å. *trans*-$[\mathrm{Re(SC_6H_5)_2(DIARS)_2}](\mathrm{C_3H_5O_2})\cdot\mathrm{H_2O}$, chemical formula $\mathrm{ReAs_4S_2O_3C_{35}H_{49}}$, crystallizes in the monoclinic space group $P2_1/c$ with $Z = 4$ and lattice parameters $a = 17.099(5)$ Å, $b = 17.515(3)$ Å, $c = 13.545(5)$ Å, $\beta = 111.41(3)°$, and $V = 3777(2)$ Å^3. Important structural parameters are Re–S = 2.298(5) Å, Re–S–C = 122(1)°, and Re–As = 2.50(1) Å. Electrochemical measurements show a reversible Re(III/II) redox couple at *ca.* −0.55 V for the *trans* complexes and *ca.* −0.52 V for the *cis* complex (both vs Ag/AgCl in TEAP/DMF). The properties of these Re(III)–DIARS complexes are compared to the properties of analogous complexes with chelating diphosphine ligands. Similar preparative reactions conducted at lower temperatures and shorter reflux times produce the Re(V) complexes $[\mathrm{ReOCl(SR)_2(DIARS)}]$, R = $\mathrm{CH_2CH_3}$ or $\mathrm{C_6H_5}$. These complexes have also been characterized by FAB mass spectroscopy, visible–UV spectroscopy, and elemental analysis. An X-ray crystal structure of $[\mathrm{ReOCl(SC_6H_5)_2(DIARS)}]$ shows that the thiolato ligands are *cis*. $[\mathrm{ReOCl(SC_6H_5)_2(DIARS)}]$, chemical formula $\mathrm{ReAs_2ClS_2OC_{22}H_{26}}$, crystallizes in the monoclinic space group $C2/c$ with $Z = 12$ and lattice parameters $a = 24.077(16)$ Å, $b = 15.725(2)$ Å, $c = 20.235(4)$ Å, $\beta = 99.88(4)°$, and $V = 7548(5)$ Å^3.

Introduction

The design of future technetium and rhenium radiopharmaceuticals relies upon the continued exploration of the basic chemistries of these metals.[4] Our studies have concentrated on the rational syntheses and complete characterizations of M(III) complexes (M = Tc, Re), the properties of which can be gradually varied. In addition, since the redox properties of technetium(III) and rhenium(III) complexes have a great deal of bearing on their biological behavior,[5] the electrochemistry of M(III) complexes has been systematically investigated.

The present study has its roots in the early work of Nyholm and Fergusson in which complexes of the formula $[\mathrm{Tc^{III}X_2D_2}]^+$, D = diphosphine or diarsine, X = halo or pseudohalo ion, were prepared.[6,7] Along these lines, we[8–15] and others[16,17] have investigated cationic thiolato $[\mathrm{Tc^{III}(SR)_2D_2}]^+$ complexes and the effects generated by variations of and on the ligands. Currently there is an interest in exploring ^{186}Re complexes that are analogous to ^{99m}Tc imaging agents and which might prove useful as companion therapeutic agents.[4d] So, along these lines, we have synthesized and characterized bis(thiolato)–Re(III) complexes with diphosphine coligands.[18,19] The natural next step is to include

---

[†] The following acronyms and abbreviations are used in this article: bdt = 1,2-benzenedithiolate; D = DIP or DIARS; DEPE = 1,2-bis(diethylphosphino)ethane; DIARS = *o*-phenylenebis(dimethylarsine); DIP = diphosphine; DMF = *N,N*-dimethylformamide; DMPE = 1,2-bis(dimethylphosphino)ethane; DPPE = 1,2-bis(diphenylphosphino)ethane; edt = 1,2-ethylenedithiolate; Et = ethyl; FAB = fast atom bombardment; NBA = *m*-nitrobenzyl alcohol; Ph = phenyl; py = pyridine; TEAP = tetraethylammonium perchlorate; tmbt = 2,3,5,6-tetramethylbenzenethiolate.

[⊗] Abstract published in *Advance ACS Abstracts*, March 1, 1994.

(1) University of Cincinnati.

(2) Wayne State University.

(3) Present address: Mallinckrodt Medical, Inc., 675 McDonnell Blvd., P.O. Box 5840, St. Louis, MO 63134.

(4) Reviews of technetium complexes as radiopharmaceuticals: (a) Deutsch, E.; Libson, K. *Comments Inorg. Chem.* **1984**, *3*, 83–103. (b) Clarke, M. J.; Podbielski, L. *Coord. Chem. Rev.* **1987**, *78*, 253–331. (c) Jones, C. L. In *Comprehensive Coordination Chemistry*; Wilkinson, G., Gillard, R. D., McCleverty, J., Eds.; Pergamon Press: Oxford, U.K., 1987; Vol. 6, p 881–1009. (d) Verbruggen, A. M. *Eur. J. Nucl. Med.* **1990**, *17*, 346–364.

(5) Deutsch, E.; Libson, K.; Vanderheyden, J.-L.; Ketring, A. R.; Maxon, H. R. *Nucl. Med. Biol.* **1986**, *13*, 465–477.

(6) Fergusson, J. E.; Nyholm, R. S. *Nature* (*London*) **1959**, *183*, 1039–1040. Fergusson, J. E.; Nyholm, R. S. *Chem. Ind.* **1960**, 347–348.

(7) Fergusson, J. E., Hickford, J. H. *J. Inorg. Nucl. Chem.* **1966**, *28*, 2293–2296. Fergusson, J. E., Hickford, J. H. *Aust. J. Chem.* **1970**, *23*, 354–461.

(8) Konno, T.; Heeg, M. J.; Deutsch, E. *Inorg. Chem.* **1988**, *27*, 4113–4121.

(9) Konno, T.; Kirchhoff, J. R.; Heineman, W. R.; Deutsch, E. *Inorg. Chem.* **1989**, *28*, 1174–1179.

(10) Konno, T.; Heeg, M. J.; Deutsch, E. *Inorg. Chem.* **1989**, *28*, 1694–1700.

(11) Konno, T.; Heeg, M. J.; Seeber, R.; Kirchhoff, J. R.; Heineman, W. R.; Deutsch, E. *Transition Met. Chem.* **1993**, *18*, 209–217.

(12) Konno, T.; Heeg, M. J.; Stuckey, J. A.; Kirchhoff, J. R.; Heineman, W. R.; Deutsch, E. *Inorg. Chem.* **1992**, *31*, 1173–1181.

(13) Konno, T.; Heeg, M. J.; Kirchhoff, J. R.; Heineman, W. R.; Deutsch, E. *J. Chem. Soc., Dalton Trans.* **1992**, 3069–3075.

(14) Okamoto, K.-I.; Kirchhoff, J. R.; Heineman, W. R.; Deutsch, E.; Heeg, M. J. *Polyhedron* **1993**, *12*, 749–757.

(15) Okamoto, K.-I.; Chen, B.; Kirchhoff, J. R.; Ho, D. M.; Elder, R. C.; Heineman, W. R.; Deutsch, E.; Heeg, M. J. *Polyhedron* **1993**, *12*, 1559–1568.

(16) Münze, R.; Abram, U.; Stach, J.; Hiller, W. *Inorg. Chim. Acta* **1991**, *186*, 151–154. Abram, U.; Beyer, R.; Mading, P.; Hoffman, I.; Münze, R.; Stach, J. *Z. Anorg. Allg. Chem.* **1989**, *578*, 229–239. Stach, J.; Abram, U.; Münze, R. *Z. Chem.* **1989**, *29*, 249–250.

(17) Rochon, F. D.; Melanson, R.; Kong, P.-C. *Inorg. Chim. Acta* **1992**, *194*, 43–50.

(18) Chang, L.; Aizawa, S.-I.; Heeg, M. J.; Deutsch, E. *Inorg. Chem.* **1991**, *30*, 4920–4927.

(19) Chang, L.; Deutsch, E.; Heeg, M. J. *Transition Met. Chem.* **1993**, *18*, 335–341.

0020-1669/94/1333-1614$04.50/0

Table 1. Crystallographic Data for *trans*-$[Re(SC_6H_5)_2(DIARS)_2](C_3H_5O_2)\cdot H_2O$ (**1**), $[ReOCl(SC_6H_5)_2(DIARS)]$ (**2**), and *trans*-$[Re(SCH_2CH_3)_2(DIARS)_2]PF_6$ (**3**)

	1	**2**	**3**
formula	$ReAs_4S_2O_3$-$C_{35}H_{49}$	$ReAs_2ClS_2$-$OC_{22}H_{26}$	$ReAs_4S_2PF_6$-$C_{24}H_{42}$
weight	1067.79	742.07	1025.58
T, °C	22	22	22
λ, Å	0.710 73	0.710 73	0.710 73
space group	*P*2$_1$/*c*	*C*2/*c*	*Pbcn*
a, Å	17.099(5)	24.077(16)	13.505(2)
b, Å	17.515(3)	15.725(2)	12.490(5)
c, Å	13.545(5)	20.235(4)	21.703(4)
β, deg	111.41(3)	99.88(4)	
V, Å^3	3777(2)	7548(5)	3361(2)
Z	4	12	4
ρ(calc), g cm^{-3}	1.878	1.959	1.861
μ, cm^{-1}	68.71	77.80	71.43
transm coeffs	0.638–0.455	0.161–0.088	0.097–0.038
R[a]	0.037	0.040	0.041
R$_w$[a]	0.041	0.040	0.039

[a] $R = (\Sigma|F_o - F_c|)/\Sigma|F_o|$; $R_w = [(\Sigma w|F_o - F_c|^2)/\Sigma wF_o^2]^{1/2}$.

Table 2. Elemental Analyses for Rhenium Complexes

compd		elemental anal % C	H	As	Re
cis-$[Re(SPh)_2(DIARS)_2]PF_6$	calcd	34.3	3.8	26.7	16.6
	found	34.5	3.8	26.7	16.9
trans-$[Re(SPh)_2(DIARS)_2]C_3H_5O_2\cdot H_2O$	calcd	39.4	4.6	28.1	17.4
	found	38.4	4.7	26.9	17.8
trans-$[Re(SPh)_2(DIARS)_2][ReO(SPh)_4]$	calcd	41.6	3.9	18.6	23.1
	found	41.3	3.9	18.3	23.3
trans-$[Re(SEt)_2(DIARS)_2]PF_6$	calcd	28.1	4.1	29.2	18.2
	found	28.0	4.1	27.8	18.2
$[ReOCl(SPh)_2(DIARS)]$	calcd	35.6	3.5	20.2	25.1
	found	35.2	3.5	20.0	24.9
$[ReOCl(SEt)_2(DIARS)]$	calcd	26.0	4.1	23.2	28.8
	found	26.0	4.1	23.2	29.5

diarsine ligands in these comparisons. With this history, we present the first studies of Re(III) complexes which contain both thiolato and diarsine ligands.

Experimental Section

Reagents. All chemicals were of reagent grade unless otherwise noted. The DIARS ligand was purchased from Strem Chemical Co., and the ammonium perrhenate, ethanethiol, and thiophenol were purchased from Aldrich Chemical Co.; all were used without further purification. Kieselgel (silica gel 60, 230–400 mesh) was obtained from Merck Co. The starting complexes, *trans*-$[ReOCl_3(PPh_3)_2]$ and $[ReO_2py_4]Cl\cdot H_2O$, were prepared by literature procedures[20] with modifications.[18] DMF from Burdick and Jackson Laboratories, Inc., and polarographic grade TEAP from G. F. Smith Chemicals were used in the electrochemical measurements.

Measurements. Elemental analyses were performed by Galbraith Laboratories, Knoxville, TN. Visible–UV spectra were recorded in methylene chloride on a Cary 210 spectrophotometer (Varian) at room temperature. FAB mass spectra were measured in the positive and negative ion modes using a VG 30-250 quadrapole mass spectrometer (VG Instruments Inc.) and *m*-nitrobenzyl alcohol (NBA) matrix at the probe temperature. Xenon was used as the primary beam gas, and the ion gun was operated at 7 kV and 1 mA. Data were generally collected over the mass range 100–1500 Da at 3 s/scan. Electrochemical measurements were made with a Bioanalytical Systems, Inc. (BAS), 100A apparatus using a glassy carbon disk working electrode, an aqueous Ag/AgCl (3 M NaCl) reference electrode, and a platinum wire auxiliary electrode. All potentials are reported *versus* this reference electrode. The electrochemical experiment was conducted in DMF with 0.5 M TEAP as supporting electrolyte, at a complex concentration of *ca.* 1 mM.

All single-crystal X-ray diffraction experiments were performed on a Nicolet R3 automated diffractometer with a graphite monochromator. Crystallographic data are summarized in Table 1. Absorption corrections were empirically derived from *ψ* scans with the program SHELXTL.[21] Structure solutions by Patterson methods and refinements used the programs of SHELX-76.[22] Neutral-atom scattering factors and corrections for anomalous dispersion were from *International Tables for X-ray Crystallography*, Vol. 4.

Synthesis. *cis*- and *trans*-$[Re(SPh)_2(DIARS)_2]^+$. A 100-mL flask containing 508 mg of $[ReOCl_3(PPh_3)_2]$ (0.6 mmol) and 30 mL of ethanol was stirred and deoxygenated with argon for 20 min in an oil bath at 100 °C. The addition of excess HSPh (0.4 mL) produced an immediate color change in the solution to deep green. Five minutes later, 0.61 g of DIARS (0.41 mL, 2.7 mmol) was injected, followed by 10 drops of NEt_3. The very dark color of the solution became red after 2 h of heating and deep red-purple after 6 h. This reaction mixture was continuously heated at 100 °C for 2 days, even though no further color change was observed. The resultant mixture was cooled and filtered, producing a dark blue-purple powder and a red filtrate.

The red solution was separated using silica gel (2.5 cm × 6 cm), eluting first with CH_2Cl_2 to remove the excess free ligands and impurities. The major component of the reaction mixture was eluted as a red band with acetone/saturated NH_4PF_6 (100 mL/10 drops to 50 mL/20 drops). This red band was concentrated and crystallized from MeOH to yield 234 mg, equivalent to 34% yield based on the starting material $[ReOCl_3(PPh_3)_2]$. Further purification by crystallization from CH_2Cl_2/acetone/toluene produced red crystals of *cis*-$[Re(SPh)_2(DIARS)_2]PF_6$, which are characterized by elemental analysis (Table 2), FAB mass spectroscopy (Table 3), and visible–UV spectroscopy (Table 4). The positive ion mode FAB mass spectrum exhibits the base peak at 977 and 975 amu corresponding to $[^{187/185}Re(SPh)_2(DIARS)_2]^+$, and the negative mode FAB mass spectrum clearly indicates the PF_6^- anion at m/z = 145 amu. The assignment of *cis* geometry is made by comparison of the visible–UV spectrum with those of known complexes and is further discussed under Results.

The blue-purple powder was extracted with 50 mL of methanol to yield a blue-purple methanolic solution and residue, each containing *trans*-$[Re(SPh)_2(DIARS)_2]^+$ associated with different anions. Diffusion of a mixture of CH_2Cl_2/CH_3CN/ether into the blue-purple solution yields 45 mg of a product (6.6% yield based on the starting material $[ReOCl_3(PPh_3)_2]$) analyzed by X-ray diffraction to be *trans*-$[Re(SPh)_2(DIARS)_2]C_3H_5O_2\cdot H_2O$. Identification of the propionate anion is not unambiguous and is discussed in the crystallography section below. This product is also characterized by elemental analysis (Table 2), FAB mass spectroscopy (Table 3), and visible–UV spectroscopy (Table 4). The position ion mode FAB mass spectrum exhibits its base peak at 977/975 amu in the appropriate isotopic ratio corresponding to $[^{187/185}Re(SPh)_2(DIARS)_2]^+$. The negative ion mode spectrum shows no obvious anionic fragment among the NBA matrix background. The residue (180 mg), after methanol extraction, was purified by crystallization with CH_2Cl_2/ether (40% yield based on the starting material $[ReOCl_3(PPh_3)_2]$). Positive ion mode FAB mass spectrometry shows the parent ions at 977 and 975 amu corresponding to the parent ions $[^{187/185}Re(SPh)_2(DIARS)_2]^+$. Negative ion mode FAB mass spectrometry shows ions at 639 and 637 amu, which corresponds to $[^{187/185}ReO(SPh)_4]^-$. An X-ray structural determination was attempted on this $[Re(SPh)_2(DIARS)_2][ReO(SPh)_4]$ material; since the refinement was problematic, it is not reported here. It did, however, confirm the identities and atom connectivities of the cation and anion and the *trans* geometry of the cation. *trans*-$[Re(SPh)_2(DIARS)_2][ReO(SPh)_4]$ is also characterized by elemental analysis (Table 2) and visible–UV spectroscopy (Table 4).

***trans*-$[Re(SEt)_2(DIARS)_2]PF_6$.** This complex is prepared analogously to $[Re(SPh)_2(DIARS)_2]^+$ except that HSEt was used instead of HSPh. The dark reaction mixture was purified on silica gel, eluting first with CH_2Cl_2 to remove impurities and then with MeOH/saturated NH_4PF_6 (100 mL/10 drops) to collect the single red band. This band was evaporated to dryness and then dissolved in a small amount of CH_2Cl_2, MeOH, and toluene. Crystals were formed after cooling the solution in the refrigerator overnight. The isolated product, $[Re(SEt)_2(DIARS)_2]PF_6$, is characterized by elemental analysis (Table 2), FAB mass spectroscopy (Table 3), visible–UV spectroscopy (Table 4), and X-ray crystallography. The +/– FAB mass spectra show the expected M^+ ion and the PF_6^- masses. The *trans* geometry is assigned by X-ray crystallography. The yield is 35%.

$[ReOCl(SPh)_2(DIARS)]$. To a suspension prepared from 0.85 g of $[ReOCl_3(PPh_3)_2]$ (1.0 mmol) in 10 mL of ethanol at 70 °C was added

---

(20) Johnson, N. P.; Lock, C. J. L.; Wilkinson, G. *J. Chem. Soc.* **1964**, 1054–1066.

(21) Sheldrick, G. M. SHELXTL. University of Göttingen, Federal Republic of Germany, 1978.

(22) Sheldrick, G. M. SHELX-76. University Chemical Laboratory Cambridge, England, 1976.

Table 3. Positive Ion Mode FAB Mass Spectral Data[a]

$[Re(SR)_2(DIARS)_2]^+$							
complex	ion (M)	fragment ions, M – ()					
		(R)	(2R)	(R,SR)	(DIARS)	(DIARS,R)	(DIARS,2R)
cis-$[Re^{III}(SPh)_2(DIARS)_2]PF_6$	977/975[b]				691/689		537/535
trans-$[Re^{III}(SPh)_2(DIARS)_2]C_3H_5O_2$	977/975[b]				691/689	613/611	537/535
trans-$[Re^{III}(SPh)_2(DIARS)_2][ReO(SPh)_4]$	977/975[b]				691/689	613/611	537/535
trans-$[Re^{III}(SEt)_2(DIARS)_2]PF_6$	881/879[b]	852/850	823/821	791/789			537/535

$[ReOCl(SR)_2(DIARS)]$							
complex	ion (M^+)	fragment ions, M – ()					
		(Cl)	(Cl,Me)	(SR)	(Cl,SR)	2SR)	(DIARS,SR,R)
$[Re^VOCl(SPh)_2(DIARS)]$	742/740[c]	707/705		633/631	598/596		
$[Re^VOCl(SEt)_2(DIARS)]$	646/644[c]	611/609	584/582			525/523	270/268

[a] The isotopic pattern due to $^{187/185}Re$ is observed as indicated. [b] Base peak. [c] The additional isotopic pattern due to $ReCl_2$ ($^{187/185}Re$, $^{37/35}Cl$) is observed, although only the Re distribution is indicated.

Table 4. Visible–UV Spectral Data for Re(III) and Re(V) Complexes in Methylene Chloride

complex	λ_{max}, nm	$\tilde{\nu}_{max}/10^3$, cm^{-1}	$\epsilon/10^3$, $M^{-1}\ cm^{-1}$
cis-$[Re(SPh)_2(DIARS)_2]PF_6$	506	19.76	11.81
	390	25.64	5.64
	312	32.05	7.66
	236	42.37	26.32
trans-$[Re(SPh)_2(DIARS)_2][ReO(SPh)_4]$	582	17.18	18.46
	486	20.58	6.00
	396	25.25	5.34
	354	28.25	10.10
	242	41.32	65.48
trans-$[Re(SPh)_2(DIARS)_2](C_3H_5O_2)$	582	17.18	21.45
	486	20.58	4.41
	358 sh	27.93	2.03
	232	43.10	26.63
trans-$[Re(SEt)_2(DIARS)_2]PF_6$	498	20.08	16.62
	322	31.06	2.95
	256	39.06	10.42
	234	42.74	13.55
$[ReOCl(SEt)_2(DIARS)_2]$	398	25.13	10.89
	358	27.93	11.86
	234	42.74	18.38
$[ReOCl(SPh)_2(DIARS)_2]$	410	24.39	4.20
	353	28.41	3.83
	240	41.67	16.70

Table 5. Electrochemical Data for *trans/cis*-$[Re(SR)_2(DIARS)_2]^+$ Complexes in 0.5 M TEAP/DMF[a,b]

complex	Re(IV/III)[c] E_{pa}	Re(IV/III)[c] E_{pc}	Re(III/II) $E^{\circ\prime}$	Re(II/I) $E^{\circ\prime}$
cis-$[Re(SPh)_2(DIARS)_2]^+$	868	738	–543	–1332
trans-$[Re(SPh)_2(DIARS)_2]^+$	1084		–476	–1560
trans-$[Re(SEt)_2(DIARS)_2]^+$	970		–763	–1786

[a] 25 °C, glassy carbon working electrode, scan rate 100 mV/s, all values in mV vs Ag/AgCl (3 M NaCl) from cyclic voltammetry. [b] $E^{\circ\prime} = (E_{pc} + E_{pa})/2$. [c] Irreversible.

a large excess of PhSH (1.0 mL, 9.5 mmol). This solution was stirred at 70 °C for 10 min, and then 858 mg of DIARS (3.0 mmol) was added. The reaction mixture was held at this temperature for 2.5 h whereupon the solution became reddish-brown. The resulting mixture was filtered although there was no precipitate at this point. The mixture was concentrated to 3 mL, and then toluene was added dropwise to precipitate a brown solid, which was recrystallized from CH_2Cl_2/toluene. $[ReOCl(SPh)_2(DIARS)]$ is characterized by elemental analysis (Table 2), FAB mass spectroscopy (Table 3), and visible–UV spectroscopy (Table 4).

$[ReOCl(SEt)_2(DIARS)]$. To a stirred solution of 420 mg $[ReO_2(py)_4]Cl\cdot 2H_2O$ (0.74 mmol) in ethanol (10 mL) at 40–60 °C was added a large excess of EtSH (0.37 mL, 5.0 mmol). After the solution was stirred for 10 min, 550 mg DIARS (2.22 mmol) was added. The resultant reaction mixture was kept at 60 °C for 1.5 h whereupon the solution became reddish brown in color. The mixture was filtered and the dark brown precipitate recrystallized from CH_2Cl_2/ether. The resulting complex $[ReOCl(SEt)_2(DIARS)]$ is characterized by elemental analysis (Table 2), FAB mass spectroscopy (Table 3), visible–UV spectroscopy (Table 4), and X-ray crystallography.

Results

Synthesis and Characterization. Initial attempts to prepare the Re(III) complexes $[Re(SPh)_2(DIARS)_2]^+$ and $[Re(SEt)_2(DIARS)_2]^+$ by methodologies optimized for the preparation of $[Re(SR)_2(DIP)_2]^+$ complexes[18,19] result instead in predominantly the Re(V) species $[ReOCl(SR)_2(DIARS)]$. Other reaction routes that were explored are (briefly) (a) $[ReOCl_4]NBu_4$/HSPh/DIARS/25 °C/overnight and (b) $[ReOCl_3(PPh_3)_2]$/HSPh/DIARS/85 °C/overnight. Here, also, the product obtained is $[ReOCl(SPh)_2(DIARS)]$. Only when the reactions employ higher temperatures (100 °C) and prolonged reaction times (48 h) does reduction of Re(V) to Re(III) occur and $[Re(SR)_2(DIARS)_2]^+$ complexes form. It appears that the $[ReOCl(SR)_2(DIARS)]$ species are reaction intermediates and that more stringent conditions are required to form $[Re(SR)_2(DIARS)_2]^+$ complexes than $[Re(SR)_2(DIP)_2]^+$ complexes.

The complexes *trans*-$[Re^{III}(SEt)_2(DIARS)_2]^+$ and *cis*- and *trans*-$[Re^{III}(SPh)_2(DIARS)_2]^+$ can be prepared by the reaction of the *trans*-$[Re^VOCl_3(PPh_3)_2]$ with excess thiol and DIARS under anaerobic conditions. A red product is obtained when R is CH_2CH_3 and the geometry is *trans* or R is C_6H_5 with *cis* geometry. A blue product is obtained with R is C_6H_5 and the arrangement is *trans*.

The reaction of $[ReOCl_3(PPh_3)_2]$ with the arenethiol, HSPh, yields both *trans*- and *cis*-$[Re(SPh)_2(DIARS)_2]^+$. The *trans* complex precipitates from the reaction mixture during cooling while the *cis* complex remains in the solution. Different salts of the *trans* complex in the blue-purple filtrate are separated by their different solubilities in methanol. The *trans* geometry of the blue-purple products have been confirmed by crystallography. The *cis* ligand arrangement of the red product is assigned by comparison of the visible–UV spectrum of red *cis*-$[Re(SPh)_2(DIARS)_2]^+$ with that of *cis*-$[Re(SPh)_2(DMPE)_2]^+$ (*cf.* λ_{max}, nm ($\epsilon/10^{-3}\ M^{-1}\ cm^{-1}$): 512 (11.45), 406 (4.87), 326 (6.27), 242 (19.73)), which has been characterized by single-crystal X-ray analysis.[19] Characterizational data are given Tables 2–4.

Electrochemistry. The three $[Re^{III}(SR)_2(DIARS)_2]^+$ complexes presented here have been further characterized by cyclic voltammetry, the results of which are summarized in Table 5. The complexes examined herein all exhibit reversible Re(III/II) and Re(II/I) couples on the basis of the criteria for reversibility outlined previously.[23] Figure 1 shows a representative CV of *cis*-$[Re(SPh)_2(DIARS)_2]^+$ over the range +1.2 to –1.8 mV. For complexes of *trans* geometry, *trans*-$[Re(SEt)_2(DIARS)_2]^+$ is harder to reduce to Re(II) than *trans*-$[Re(SPh)_2(DIARS)_2]^+$ by

---

(23) Kirchhoff, J. R.; Heineman, W. R.; Deutsch, E. *Inorg. Chem.* **1987**, *26*, 3108–3113.

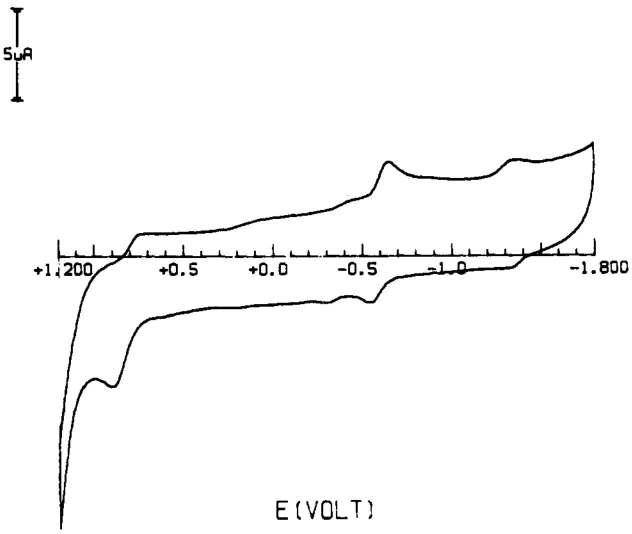

Figure 1. Cyclic voltammogram of 0.713 mM *cis*-$[\text{Re(SPh)}_2(\text{DIARS})_2]^+$ in 0.5 M TEAP/DMF at a glassy-carbon electrode. The scan rate is 100 mV/s.

287 mV. This is in agreement with our previous observations on alkyl *vs* aryl substituents in related complexes.[18,23,24] Table 5 shows that the *trans*-$[\text{Re(SPh)}_2(\text{DIARS})_2]^+$ complex is easier to reduce to Re(II) than *cis*-$[\text{Re(SPh)}_2(\text{DIARS})_2]^+$, and this is in contrast to our work with *cis*- and *trans*-$[\text{Re(SPh)}_2(\text{DMPE})_2]^+$.[19]

Crystallography. $[\text{Re(SPh)}_2(\text{DIARS})_2](\text{C}_3\text{H}_5\text{O}_2)\cdot\text{H}_2\text{O}$. The structure consists of two independent half-cations, an anion, and a water solvent molecule. Each Re atom occupies a crystallographic inversion center. Table 6 contains the atomic positions, and Table 7 lists selected bond lengths and angles. Figure 2 shows one of the independent cations. The benzenethiolato ligands are arranged *trans*. Deviations from octahedral geometry are primarily 2-fold: (i) the acute DIARS chelate bite angles (82.8(2)° average) and (ii) the nonorthogonality of the S–Re vector to the ReAs_4 basal plane (83.6(8)° average). Metal–ligand bond lengths are normal for Re^{III} at 2.298(5) Å for Re–S and 2.497(10) Å for Re–As. The DIARS ligands are nearly planar; there is a 4.3(8) and 3.6(9)° bend between the ReAs_2 plane and the associated phenyl plane. The phenyl rings, both on sulfur and in the DIARS ligand, were refined as rigid bodies with individual anisotropic thermal parameters.

It was expected that the anion would be PF_6^-, but this turned out not to be the case. Instead it is a light atom molecule of uncertain identity, composed of five non-hydrogen atoms with relatively short bond lengths. The $-\text{CO}_2^-$ or $-\text{NO}_2^-$ portion of the anion participates in hydrogen bondinging with the water solvent molecule in linear chains. The differentiation of C, N, or O atoms in the anion region cannot be certain in the presence of heavy atoms. Since this anion was oxidatively generated in the preparation and not deliberately introduced, there are multiple possibilities for its identity. It could be propionate, propenoate, glycollate, peracetate, glyoxylate, or others. A number of attempts were made to model the exact identity of the anion, with the result that none modeled the region any better than the others. Lacking specific knowledge, it has been assigned to be propionate with reference to the elemental analysis. That this moiety is negatively charged, and not a neutral solvent molecule, has been decided on the basis of Re–S and Re–As bond lengths, which are quite diagnostic for Re^{III}. By analogy with Tc, we would predict Re^{II}–S ~ 2.41 Å and Re^{II}–As ~ 2.47 Å.

$[\text{ReOCl(SPh)}_2(\text{DIARS})]$. The structure consists of neutral molecules with no solvent or charged ions in the lattice. One independent molecule is well behaved with Re1 in a general position. The other independent half-molecule containing Re2 is constrained by symmetry to occupy a 2-fold rotation axis in space group *C*2/*c*. DIARS and the two SPh ligands around Re2 obey this 2-fold symmetry, but space group *C*2/*c* requires an equivalence, and therefore disorder, in the axial ligands. Placing the molecules in the acentric space group Cc removes the 2-fold symmetry, but axial disorder was still evident around Re2 and full refinement was impossible due to many very high (>0.9) correlation coefficients. A satisfactory description of the molecule at this site was obtained in *C*2/*c* with each axial site composed of $^1/_2$ oxygen and $^1/_2$ chloride atom. At this point a ΔF map continued to show 10 e⁻ very near Re2. By examination of the behaved molecule, it was known that Re would not occupy the As_2S_2 plane but would be displaced ~0.3 Å toward the -yl oxygen

Table 6. Atomic Positional Parameters and *U*(eq) Values for $[\text{Re(SC}_6\text{H}_5)_2(\text{DIARS})_2](\text{C}_3\text{H}_5\text{O}_2)\cdot\text{H}_2\text{O}$[a]

atom	*x*	*y*	*z*	*U*(eq), Å²
Re1	1.00000	–1.00000	0.00000	0.0249(3)
As1	0.89633(8)	–0.95700(8)	0.0786(1)	0.0288(5)
As2	0.98505(9)	–1.12451(7)	0.0811(1)	0.0319(6)
S1	1.1179(2)	–0.9656(2)	0.1409(3)	0.039(1)
C1	1.1171(5)	–0.9488(5)	0.2693(5)	0.032(5)
C2	1.1651(5)	–0.8876(5)	0.3254(5)	0.046(6)
C3	1.1641(5)	–0.8683(5)	0.4249(5)	0.060(8)
C4	1.1149(5)	–0.9102(5)	0.4681(5)	0.061(8)
C5	1.0669(5)	–0.9714(5)	0.4119(5)	0.056(7)
C6	1.0680(5)	–0.9907(5)	0.3125(5)	0.047(6)
C7	0.7848(8)	–0.9285(8)	–0.017(1)	0.038(6)
C8	0.9171(9)	–0.8698(7)	0.176(1)	0.043(6)
C9	0.8679(5)	–1.0425(4)	0.1503(6)	0.033(5)
C10	0.8070(5)	–1.0342(4)	0.1955(6)	0.046(6)
C11	0.7828(5)	–1.0970(4)	0.2410(6)	0.050(7)
C12	0.8196(5)	–1.1681(4)	0.2413(6)	0.047(7)
C13	0.8805(5)	–1.1765(4)	0.1961(6)	0.036(6)
C14	0.9047(5)	–1.1137(4)	0.1506(6)	0.027(5)
C15	0.937(1)	–1.2079(8)	–0.013(1)	0.062(8)
C16	1.0819(9)	–1.1757(8)	0.187(1)	0.048(6)
Re2	0.50000	–1.00000	0.50000	0.0240(3)
As3	0.42768(8)	–1.09877(7)	0.3626(1)	0.0295(5)
As4	0.56984(8)	–0.96751(8)	0.3734(1)	0.0299(5)
S2	0.3924(2)	–0.9133(2)	0.4325(3)	0.034(1)
C17	0.3725(5)	–0.8687(5)	0.3069(6)	0.034(6)
C18	0.3510(5)	–0.9103(5)	0.2129(6)	0.048(6)
C19	0.3339(5)	–0.8724(5)	0.1167(6)	0.064(8)
C20	0.3382(5)	–0.7929(5)	0.1145(6)	0.071(9)
C21	0.3597(5)	–0.7513(5)	0.2085(6)	0.064(8)
C22	0.3768(5)	–0.7893(5)	0.3047(6)	0.050(7)
C23	0.3062(8)	–1.1040(7)	0.303(1)	0.036(6)
C24	0.454(1)	–1.2037(7)	0.398(1)	0.055(7)
C25	0.4643(5)	–1.0867(5)	0.2436(6)	0.040(6)
C26	0.4308(5)	–1.1333(5)	0.1545(6)	0.045(6)
C27	0.4610(5)	–1.1282(5)	0.0720(6)	0.058(7)
C28	0.5247(5)	–1.0765(5)	0.0785(6)	0.051(7)
C29	0.5583(5)	–1.0299(5)	0.1675(6)	0.049(7)
C30	0.5281(5)	–1.0349(5)	0.2501(6)	0.028(5)
C31	0.6903(7)	–0.9857(8)	0.418(1)	0.043(6)
C32	0.5640(9)	–0.8677(7)	0.308(1)	0.045(7)
O1	0.2759(7)	–0.1584(6)	0.8044(9)	0.079(6)
O2	1.7530(7)	–0.7584(7)	1.386(1)	0.086(4)
O3	1.7141(8)	–0.7535(7)	1.5215(9)	0.087(4)
C33	1.768(1)	–0.778(1)	1.485(2)	0.087(6)
C34	1.827(1)	–0.8154(9)	1.535(1)	0.049(4)
C35	1.875(1)	–0.840(1)	1.488(2)	0.118(8)

[a] $U(\text{eq}) = {}^1/_3\sum_i\sum_j U_{ij}a_i^*a_j^*\mathbf{a}_i\cdot\mathbf{a}_j$.

Table 7. Selected Bond Lengths (Å) and Angles (deg) for $[\text{Re(SC}_6\text{H}_5)_2(\text{DIARS})_2](\text{C}_3\text{H}_5\text{O}_2)\cdot\text{H}_2\text{O}$

Re1–As1	2.494(1)	Re2–As3	2.511(1)
Re1–As2	2.496(1)	Re2–As4	2.487(1)
Re1–S1	2.293(3)	Re2–S2	2.303(3)
S1–C1	1.769(8)	S2–C17	1.787(8)
Re1–S1–C1	122.8(2)	Re2–S2–C17	120.9(3)
As1–Re1–As2	82.72(4)	As3–Re2–As4	82.94(4)
As1–Re1–S1	96.39(7)	As3–Re2–S2	93.11(9)
As2–Re1–S1	93.7(1)	As4–Re2–S2	95.19(8)

---

(24) Libson, K.; Barnett, B. L.; Deutsch, E. *Inorg. Chem.* **1983**, *22*, 1695–1703.

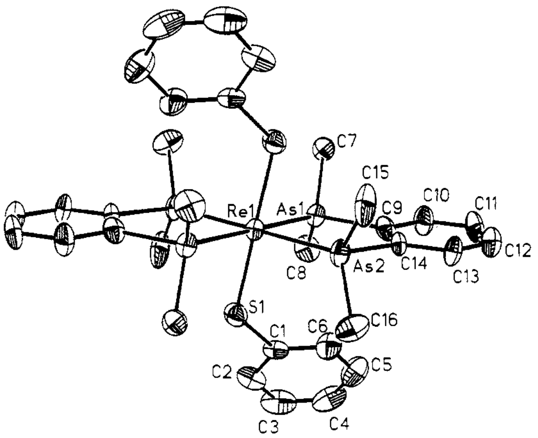

Figure 2. Perspective view of one of the independent [Re(SC_6H_5)$_2$(DIARS)$_2$]$^+$ cations. The Re occupies a crystallographic inversion center. Ellipsoids here and in all figures represent 50% probability.

atom. Thus, Re2 was allowed to refine off the crystallographic 2-fold axis to yield a clean ΔF map in this region, smaller Re2 temperature parameters (U_{iso}(Re2) ~ 0.038 with Re2 slightly off the 2-fold vs U_{iso}(Re2) ~ 0.069 with Re2 constrained to lie on the 2-fold axis), and improved Re2–O2 and Re2–Cl2 distances. Comparisons of precise structural parameters with those of other structures should, of course, be made with reference to the ordered molecule of this structure.

Table 8 contains the atomic parameters. Figure 3 illustrates the labeling the geometry of the molecule. Table 9 lists selected bond lengths and angles for the ordered molecule. The Re atom is in a 6-coordinate environment that is substantially distorted from octahedral geometry. The atoms making up the basal plane (As1, As2, S1, S2) are planar, and Re1 lies 0.309 Å out of this plane toward the doubly bound oxygen, O1. The axial ligands, O1 and Cl1, are not orthogonal to the basal plane but are canted 79(1) and 80(1)°, respectively, toward the DIARS ligand due. The Cl–Re–O angle is 159.4(2)°, which is a distortion of >20° from octahedral angles. Mean metal coordination bond lengths are Re^{V}–S = 2.326(7) Å and Re^{V}–As = 2.551(4) Å. The Re–S–C angle is 113.4(3)°. The DIARS ligand is slightly bent, having a 6.4(2)° dihedral angle between the ReAs$_2$ plane and its aromatic ring. The DIARS bite angle is normal at 81.24(2)°.

[Re(SEt)$_2$(DIARS)$_2$]PF$_6$. The structure consists of one independent half-cation and one independent half-anion. The cation occupies a crystallographic inversion center in the unit cell. The PF$_6$ anion occupies a general site in the cell at half-occupany only. Although only half of these anion sites contain an anion, it is unlikely that the remaining half are empty; rather these remaining sites probably contain solvent (CH_2Cl_2 and/or H_2O) molecules. The difference electron density maps in this region were ill-defined. Around the phosphorus atom was a sphere of gradually modulating electron density. Assignment of definite positions for the fluorine atoms was not useful due to the evident disorder of the F atoms and (probably) solvent molecules. In an attempt to model this region, 12 F atoms were placed with partial occupancies to sum to 3 whole F atoms (representing $^1/_2$ PF$_6$ anion). The F atoms were held invariant after some cycles of refinement since convergence was impossible. The remainder of the model converged easily and the cation is well behaved.

Table 8. Atomic Positional Parameters and *U*(eq) Values for [ReOCl(SC_6H_5)$_2$(DIARS)][a]

atom	*x*	*y*	*z*	*U*(eq), Å^2
Re1	0.13784(2)	0.51223(2)	0.08173(2)	0.0397(1)
As1	0.13439(4)	0.51800(5)	−0.04470(4)	0.0393(3)
As2	0.13820(4)	0.35263(6)	0.05812(4)	0.0446(3)
Cl1	0.2351(1)	0.4802(2)	0.0676(1)	0.064(1)
S1	0.1613(1)	0.6543(1)	0.1046(1)	0.0575(9)
S2	0.1666(1)	0.5109(2)	0.1971(1)	0.064(1)
O1	0.0662(3)	0.5073(4)	0.0698(3)	0.059(2)
C1	0.1427(4)	0.7236(5)	0.0331(4)	0.052(3)
C2	0.1837(4)	0.7797(6)	0.0210(5)	0.061(3)
C3	0.1702(5)	0.8370(6)	−0.0317(6)	0.076(4)
C4	0.1168(6)	0.8371(6)	−0.0693(5)	0.076(4)
C5	0.0772(5)	0.7817(7)	−0.0559(5)	0.068(4)
C6	0.0892(4)	0.7238(6)	−0.0037(5)	0.053(3)
C7	0.1745(5)	0.4070(6)	0.2309(4)	0.056(3)
C8	0.2267(5)	0.3764(6)	0.2546(5)	0.066(4)
C9	0.2347(6)	0.2989(8)	0.2853(5)	0.081(4)
C10	0.1878(7)	0.2504(7)	0.2914(5)	0.081(4)
C11	0.1357(6)	0.2789(8)	0.2685(5)	0.077(4)
C12	0.1286(5)	0.3578(8)	0.2379(5)	0.076(4)
C13	0.1886(4)	0.5859(6)	−0.0795(4)	0.058(3)
C14	0.0637(4)	0.5487(6)	−0.1017(4)	0.065(3)
C15	0.1456(4)	0.4042(5)	−0.0774(4)	0.042(3)
C16	0.1446(4)	0.3340(5)	−0.0352(4)	0.046(3)
C17	0.1485(4)	0.2538(6)	−0.0609(4)	0.059(3)
C18	0.1534(5)	0.2426(6)	−0.1265(5)	0.069(4)
C19	0.1538(5)	0.3111(7)	−0.1683(5)	0.066(4)
C20	0.1504(4)	0.3928(6)	−0.1435(4)	0.056(3)
C21	0.0685(5)	0.2950(6)	0.0637(5)	0.068(4)
C22	0.1947(5)	0.2758(5)	0.1033(5)	0.065(3)
Re2	−0.00982(7)	0.99075(4)	0.23983(8)	0.0394(5)
As3	0.03502(4)	0.86864(5)	0.18575(4)	0.0475(3)
S3	0.0331(1)	1.1034(1)	0.1946(1)	0.062(1)
O2	−0.073(2)	0.974(2)	0.182(2)	0.120(6)
Cl2	0.0758(4)	0.9630(6)	0.3177(6)	0.057(2)
C23	0.0840(4)	1.0713(5)	0.1449(5)	0.053(3)
C24	0.1403(5)	1.0697(6)	0.1740(6)	0.072(4)
C25	0.1808(5)	1.0520(7)	0.1362(7)	0.088(4)
C26	0.1670(6)	1.0366(8)	0.0710(8)	0.103(4)
C27	0.1098(7)	1.0371(7)	0.0411(6)	0.097(4)
C28	0.0686(5)	1.0562(6)	0.0775(5)	0.074(4)
C29	0.1140(4)	0.8553(5)	0.1869(5)	0.068(3)
C30	0.0031(5)	0.8558(7)	0.0930(5)	0.079(4)
C31	0.0141(4)	0.7629(5)	0.2237(4)	0.042(3)
C32	0.0301(4)	0.6847(5)	0.1985(4)	0.055(3)
C33	0.0157(4)	0.6100(5)	0.2242(5)	0.067(4)

[a] $U(\mathrm{eq}) = {}^1/_3\sum_i\sum_j U_{ij}a_i^*a_j^*\mathbf{a}_i\cdot\mathbf{a}_j$.

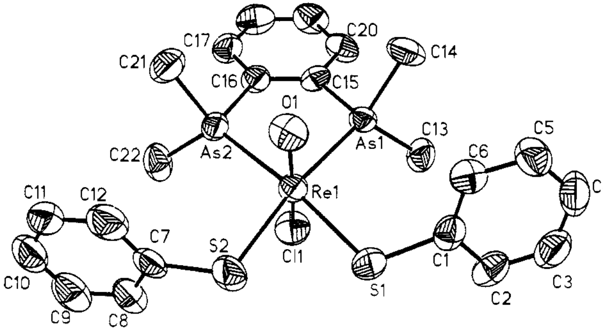

Figure 3. Geometry and labeling of [ReOCl(SC_6H_5)$_2$(DIARS)].

The Re coordination geometry is *trans*. Table 10 contains the atomic positions, and Table 11 lists the important bond lengths and angles in the cation. Symmetry requires that the Re ion occupy the As$_4$ plane. The Re–S bond vector is nearly orthogonal, 87.7(5)°, to this plane. The most severe distortion from octahedral geometry is the DIARS bite angle (81.33(3)°). The Re^{III}–S length is 2.284(3) Å, and the Re–S–C angle is 119.5(4)°. The Re^{III}–As length averages 2.480(4) Å. There is a small bend in the DIARS ligand of 12.2(9)° between the ReAs$_4$ plane and the DIARS aromatic ring. Figure 4 presents a perspective view of the cation.

Discussion

Preparation. Attempts to prepare Re^{III}–DIARS–thiolato complexes by a general method which was optimized for the preparation of [Re(SR)$_2$(DIP)$_2$]$^+$ complexes results primarily in the metathesis product [Re^{V}OCl(SR)$_2$(DIARS)] rather than the desired reduction product [Re^{III}(SR)$_2$(DIARS)$_2$]$^+$. This indicates

Table 9. Selected Bond Lengths (Å) and Angles (deg) for [$ReOCl(SC_6H_5)_2$(DIARS)]

Re1–As1	2.5470(7)	Re1–S2	2.319(2)
Re1–As2	2.555(1)	Re1–O1	1.702(6)
Re1–Cl1	2.461(3)	S1–C1	1.805(8)
Re1–S1	2.332(2)	S2–C7	1.769(9)
Re1–S1–C1	113.6(3)	As2–Re1–S2	99.76(6)
Re1–S2–C7	113.1(3)	As2–Re1–O1	88.0(2)
As1–Re1–As2	81.24(2)	Cl1–Re1–S1	90.94(9)
As1–Re1–Cl1	76.00(6)	Cl1–Re1–S2	89.41(9)
As1–Re1–S1	97.49(5)	Cl1–Re1–O1	159.4(2)
As1–Re1–S2	164.67(8)	S1–Re1–S2	77.78(8)
As1–Re1–O1	90.1(2)	S1–Re1–O1	106.1(2)
As2–Re1–Cl1	75.11(6)	S2–Re1–O1	105.2(2)
As2–Re1–S1	165.91(8)		

Table 10. Atomic Positional Parameters and *U*(eq) Values for [$Re(SCH_2CH_3)_2(DIARS)_2]PF_6$[a]

atom	*x*	*y*	*z*	*U*(eq), Å^2
Re1	0.50000	0.00000	0.50000	0.0416(1)
As1	0.51749(7)	0.16962(8)	0.44121(4)	0.0499(3)
As2	0.34773(7)	–0.01268(9)	0.43685(4)	0.0525(3)
S1	0.4092(2)	0.0908(2)	0.5718(1)	0.059(1)
C1	0.6430(7)	0.2050(9)	0.4021(5)	0.074(5)
C2	0.4865(8)	0.3028(9)	0.4818(5)	0.080(5)
C3	0.4248(7)	0.1716(9)	0.3737(4)	0.051(4)
C4	0.4280(8)	0.2485(9)	0.3281(4)	0.060(4)
C5	0.3588(9)	0.248(1)	0.2808(5)	0.075(5)
C6	0.288(1)	0.172(1)	0.2790(5)	0.077(5)
C7	0.2846(8)	0.092(1)	0.3233(4)	0.068(4)
C8	0.3513(7)	0.0914(9)	0.3712(4)	0.055(4)
C9	0.2231(7)	0.022(1)	0.4745(5)	0.080(5)
C10	0.3159(8)	–0.1453(9)	0.3954(5)	0.077(5)
C11	0.432(1)	0.067(1)	0.6525(4)	0.085(5)
C12	0.355(1)	0.109(1)	0.6917(6)	0.119(7)
P1	0.0402(4)	0.0622(5)	0.1714(3)	0.069(2)
F1	0.11718	0.11851	0.14247	0.138(6)
F2	–0.04696	0.00245	0.20452	0.119(7)
F3	0.07406	–0.02302	0.14210	0.14(1)
F4	0.00747	0.15041	0.21125	0.17(1)
F5	–0.01878	0.06522	0.12230	0.131(8)
F6	0.10426	0.00292	0.21986	0.12(1)
F7	0.14985	0.03106	0.13963	0.10(2)
F8	–0.03286	0.14349	0.14156	0.10(1)
F9	0.10812	–0.03985	0.17380	0.09(1)
F10	–0.02284	–0.00206	0.14115	0.12(2)
F11	0.03104	0.01427	0.10690	0.07(1)
F12	0.07821	0.08767	0.23397	0.14(2)

[a] $U(eq) = {}^1/_3\sum_i\sum_j U_{ij}a_i^*a_j^*\mathbf{a}_i\cdot\mathbf{a}_j$.

Table 11. Selected Bond Lengths (Å) and Angles (deg) for [$Re(SCH_2CH_3)_2(DIARS)_2]^+$

Re1–As1	2.484(1)	Re1–S1	2.284(3)
Re1–As2	2.4763(9)	S1–C11	1.80(1)
Re1–S1–C11	119.5(4)	As2–Re1–S1	87.89(7)
As1–Re1–As2	81.33(3)	S1–C11–C12	113.3(9)
As1–Re1–S1	88.72(7)		

that reduction of Re(V) to Re(III) is not facile even when a 10-fold excess of thiol and 3-fold excess of DIARS are employed. Raising the reaction temperature to 100 °C and extending the reaction time to 48 h provides good yields of the Re(III)-thiolato–DIARS products. These synthetic observations imply that DIARS ligates to Re(V) before reduction to Re(III) has occurred and that the resulting Re(V)–DIARS intermediate is more stable and less reactive to reduction than the analogous Re(V)–DIP intermediates.[18]

In the successful preparation of the alkanethiolato complex [$Re(SEt)_2(DIARS)_2]^+$, only the *trans* isomer is apparently formed. This is consistent with the product distribution observed in the preparations of alkanethiolato complexes within the Re^{III}–DIP and Tc^{III}–DIP systems (DIP = DMPE, DEPE, DPEE).[8,9,12,14,18] In the benzenethiolato case, three products, *cis*-[$Re(SPh)_2(DIARS)_2]PF_6$, *trans*-[$Re(SPh)_2(DIARS)_2]C_3H_5O_2$, and *trans*-[$Re(SPh)_2(DIARS)_2][ReO(SPh)_4]$, are isolated from this one-pot reaction. The *cis*/*trans* ratio is 4:3. This mixture of isomers is not observed in the preparation of arenethiolato complexes of the Re^{III}–DEPE or Re^{III}–DPPE systems wherein only *trans* complexes result.[18] Analogous *cis*/*trans* mixtures are, however, produced during the synthesis of arenethiolato complexes of the Re^{III}–DMPE and Tc^{III}–DMPE systems.[11,19] However, in the pair of isomers *cis*- and *trans*-[$Tc(SC_6H_4\text{-}X)_2(DMPE)_2$], the *trans* form usually cannot be obtained as a pure product due to its rapid isomerization to the *cis* isomer. Further discussion of the relative occurrence of *cis*/*trans* isomers is presented in the crystallography discussion section below. The appearance of [$Re(SPh)_2(DIARS)_2][ReO(SPh)_4]$ in the reaction mixture suggests the occurrence of a side reaction pathway wherein the very stable 5-coordinate [$Re^VO(SPh)_4]^-$ ion is formed by substitution onto the starting material; this Re(V) anion appears to be resistant to subsequent reduction to Re(III).

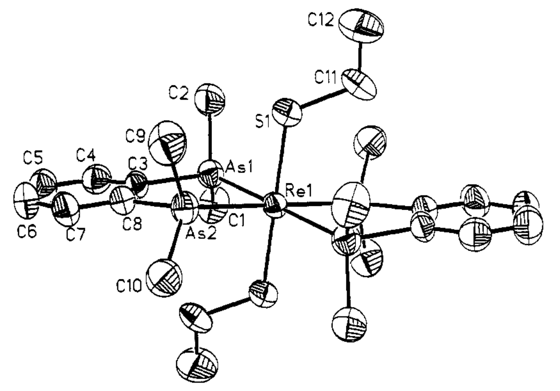

Figure 4. Perspective view of [$Re(SCH_2CH_3)_2(DIARS)_2]^+$. The Re atom occupies a crystallographic inversion center.

Visible–UV Spectra. The spectral transitions exhibited by Re–thiolates with DIARS ligands (Table 4) are similar to those of Re–thiolates with diphosphine ligands. Typically there are 2–3 intense absorptions in the visible region assigned to be $S(\pi) \rightarrow Re(t_{2g})$ charge-transfer (CT) transitions. The UV region contains the CT transitions originating on either P or As. In addition, those thiolato ligands containing aromatic moieties (e.g., SPh) exhibit very intense ($\epsilon > 25 \times 10^3$ M^{-1} cm^{-1}) $\pi \rightarrow \pi^*$ ligand transitions which can obscure the lower intensity P/As → Re CT bands.

The visible spectrum of *trans*-[$Re(SEt)_2(DIARS)_2]PF_6$ exhibits two intense absorptions, the most prominent at 498 nm ($\epsilon = 16.6 \times 10^3$ M^{-1} cm^{-1}) and a less intense peak at 322 nm ($\epsilon = 2.9 \times 10^3$ M^{-1} cm^{-1}). Both the wavelengths and the associated extinction coefficients are similar to those observed in the spectrum of *trans*-[$Re(SEt)_2(DEPE)_2]^+$: 509 nm (20.96 × 10^3 M^{-1} cm^{-1}) and 318 nm (2.21 × 10^3 M^{-1} cm^{-1}).[18] This pattern of visible absorption bands is diagnostic for the *trans* isomer of these alkanethiolato complexes.

The spectrum reported for *trans*-[$Re(SPh)_2(DIARS)_2][ReO(SPh)_4]$ has absorptions in common with *trans*-[$Re(SPh)_2(DIARS)_2](C_3H_5O_2)$ but is complicated by additional contributions from the [$ReO(SPh)_4]^-$ anion. *trans*-[$Re(SPh)_2(DIARS)_2](C_3H_5O_2)$ exhibits an absorption spectrum altogether similar to that of other *trans*-[$Re(SPh)_2(DIP)_2]^+$ complexes.[18,19] It is instructive to list the energy of the most intense visible peak through a variety of phosphine/arsine ligands; i.e., for *trans*-[$Re(SPh)_2(D)_2]^+$, *E*(DEPE) > *E*(DMPE) > *E*(DIARS) > *E*(DPPE) (569, 572, 582, and 607 nm, respectively). This series shows that the energy of this transition decreases with increasing π-acceptor ability of the chelating P/As ligand, consistent with assigning this band as arising from a $S(\pi) \rightarrow Re(t_{2g})$ transition.

When these [$Re(SPh)_2(DIP)_2]^+$ complexes adopt a *cis* configuration, the resulting spectra are markedly different from that observed for the *trans* configuration and are easily distinguishable.

Table 12. Comparative Re^{III} and Tc^{III} Structural Parameters

ref	M–S, Å	M–S–C, deg	M–As or M–P, Å	bite angle, deg	S–M vector to basal plane, deg
			trans-$[Re(SC_6H_5)_2(DIARS)_2]^+$		
a	2.298(5)	122(1)	2.50(1)	82.8(2)	83.6(8)
			trans-$[Re(SCH_2CH_3)_2(DIARS)_2]^+$		
a	2.284(3)	119.5(4)	2.480(4)	81.33(3)	87.7(5)
			trans-$[Tc(SCH_3)_2(DIARS)_2]^+$		
12	2.292(2)	118.9(2)	2.496(2)	82.39(2)	87.5(4)
			cis-$[Re(SPh)_2(DMPE)_2]^+$		
19	2.293(4)	118.5(4)	2.415(3) (*trans* P) 2.486(4) (*trans* S)	80.4(5)	NA
			trans-$[Re(SC_6H_5)_2(DEPE)_2]^+$		
18	2.305(1)	127.8(1)	2.45(2)	81.47(4)	81.0(4)
			trans-$[Re(SC_6H_5)_2(DPPE)_2]^+$		
18	2.303(3)	128.7(3)	2.47(1)	80.5(5)	80.3(6)
			trans-$[Re(SC_6H_4\text{-}p\text{-}CH_3)_2(DEPE)_2]$		
18	2.321(1)	125.7(2)	2.45(3)	80.78(4)	86.6(4)

[a] This work.

In *cis*-$[Re(SPh)_2(DIARS)_2]^+$ there are three visible absorptions, the most intense of which is located at much lower wavelength (506 nm) than in the *trans* analog (582 nm). Besides the shorter wavelength of the most intense visible band, the appearance of the absorption at *ca.* 400 nm is diagnostic for *cis* geometry in this series of complexes. Similar absorption characteristics have been noted for *cis*- and *trans*-$[Tc(SR)_2(DIP)_2]^+$ complexes, except that spectral transitions are lower in energy for technetium(III) relative to rhenium(III) complexes.[11,12] Since Tc(III) is a better oxidant than Re(III),[23] this observation is again consistent with assigning these bands as arising from S (π) → Re (t_{2g}) transitions.

Crystallography. The structures reported herein represent the first Re–DIARS complexes to be structurally characterized. Recently we have reported the synthesis and characterization of a number of Tc–DIARS complexes[12] as well as Re–diphosphine–thiolato complexes,[18,19] and Table 12 collects these important structural parameters. Re and Tc complexes are often indistinguishable in their coordination geometry[11,19,25,26] making certain complexes of these nuclides useful in the field of diagnostic and therapeutic nuclear medicine.[4d] Therefore it is instructive to consider analogous Re and Tc complexes as a single group when elucidating structural properties.

One interesting property of $[M^{III}(SR)_2DIP_2]^+$ complexes (M = Tc, Re) is the relative occurence of *trans* and *cis* isomers. It has been observed that these complexes form only the *trans* isomer when DIP = DEPE or DPPE.[8,9,18] Structural analyses indicate that the *trans* geometry is sterically favored by these larger DIP ligands. This geometry may also allow more effective M → P back-bonding since the phosphine ligand is not *trans* to the *trans*-labilizing SR ligand which can significantly increase the M–P bond length.[11] When DIP = DMPE, the *trans* isomer is still generated exclusively when SR is an alkanethiolato ligand,[8,9] but the *cis* isomer predominates when SR is an arenethiolato ligand.[11,19] The *cis* geometry provides more room for the SR ligands at the expense of the DIP ligands. *Cis* complexes typically possess M–S–C angles closer to the predicted tetrahedral value indicating less steric crowding at the thiolate. Thus, for the $[M^{III}(SR)_2(DIP)_2]^+$ complexes, *cis* geometry is favored when smaller DIP ligands (*i.e.*, DMPE) are combined with larger SR ligands (e.g., arenethiolates).

Related DIARS complexes behave similarly but with some differences. In $[Mn^{III}(SR)_2(DIARS)_2]^+$ (M = Tc, Re) complexes,[12] only the *trans* isomer is formed with alkanethiolato ligands. This is predicted since the alkanethiolato ligands have few steric constraints in the *trans* positions. However both *cis* and *trans* isomers are produced with arenethiolato ligands. Since DIARS is a more compact ligand than DIP, it can easily form *cis* complexes. It also presents less of a steric burden to the *trans*-arenethiolato ligands in *trans* complexes. For comparison, the M–S–C angle in *trans*-$[Re(SPh)_2(DIARS)_2]^+$ at 122(1)° is less strained than that in *trans*-$[Re(SPh)_2(DEPE)_2]^+$ (127.8(1)°) or in *trans*-$[Re(SPh)_2(DPPE)_2]^+$ (128.7(3)°). Therefore it is consistent with our steric analysis that both *cis* and *trans* isomers of $[M(SPh)_2(DIARS)_2]^+$ are formed.[12]

From Table 12 it is seen that the average Re^{III}–SPh length is 2.300(5) Å, having no dependence on whether the coligands are DMPE, DEPE, DPPE, or DIARS. This is in agreement with data on Tc complexes,[11] in which a summary of a mixed group of *cis*- and/or *trans*-$[Tc(SR)_2(DMPE)_2]^+$ structures shows Tc^{III}–S in the range 2.29–2.30 Å including both alkane- and arenethiolato ligands. *trans*-$[Re(SEt)_2(DIARS)_2]^+$ has Re–S = 2.284(3) Å, which is close to this range. In general the alkanethiolato complexes of Table 12, $[Re(SEt)_2(DIARS)_2]^+$ and $[Tc(SCH_3)_2(DIARS)_2]^+$, show less crowding in the regions of the thiolato ligands. These M–S–C angles are smaller than those observed in complexes which contain the larger arenethiolato ligands in the *trans* configuration, and the M–S bond vectors are more nearly orthogonal to the basal plane where applicable. Less crowding around the thiolato ligand is also evident in the *cis*-$[Re(SPh)_2(DMPE)_2]^+$ complex. The two Re^{III} structures reported herein show a mean Re^{III}–As distance of 2.49(1) Å, identical within error to the Tc^{III}–As length of 2.496(2) Å in $[Tc(SCH_3)_2(DIARS)_2]^+$. From these data, it is clear that there is no substantive structural difference between Tc and Re complexes of the type $[M^{III}(SR)_2(D)_2]^+$. This implies, to a first order, that there is no substantive difference in the bonding scheme and that bonding is predominantly driven by π-interactions.

In $[Re^VOCl(SPh)_2(DIARS)]$, the Re^V–As length is slightly longer than above at 2.551(4) Å. A longer Re–As length is expected with higher Re oxidation state since DIARS is an effective π-back-bonding ligand. The Re^V-S length of 2.326(7) Å is in the range of values 2.31–2.34 Å found for $[Re^VO(SC_6H_5)_4]^-$,[27] $[Re^VO(edt)_2]^-$,[28] and $[Re^VO(bdt)_2]^-$.[28] These Re^V–S lengths are slightly longer than the typical 2.30 Å found for Re^{III}–S, implying some π-back-bonding in the Re(III) complexes. The Re–S–C angle is 113.4(3)°, lower than generally found in 6-coordinate benzenethiolato complexes and comparable to that in 5-coordinate $[ReO(SC_6H_5)_4]^-$ [27] (114(2)° average) and $[Tc(tmbt)_3(MeCN)_2]$[29] (112(3)° average). Although the axial ligands are bent, the Re–Cl length (2.461(3) Å) and Re═O length (1.702(6) Å) are similar to those in $[ReOCl_3(PPhEt_2)_2]$ in which a linear Cl–Re═O core is found (Re–Cl = 2.445 Å, Re═O = 1.660 Å, Cl–Re═O = 177.0°).[30]

Electrochemistry. The electrochemical studies in 0.5 M TEAP/DMF have been purposely conducted under the same conditions as in our previous reports to allow facile comparisons between series of related complexes. Table 13 summarizes the M(III/II) potentials for groups of analogous complexes. The following generalities can be observed. (i) In *trans*-$[M^{III}(SR)_2D_2]^+$ complexes, the DIARS complexes are easier to reduce than the DMPE complexes. In fact, previous studies[23] of *trans*-$[TcCl_2D_2]^+$ and *trans*-$[ReCl_2D_2]^+$ have established the ordering of M(III/II) potentials, DPPE > DIARS > DMPE > DEPE, such that

---

(25) Vanderheyden, J.-L.; Heeg, M. J.; Deutsch, E. *Inorg. Chem.* **1985**, *24*, 1666–1673.

(26) Vanderheyden, J.-L.; Ketring, A. R.; Heeg, M. J.; Roecker, L.; Motz, P.; Whittle, R.; Elder, R. C.; Deutsch, E. *Inorg. Chem.* **1984**, *24*, 3184–3191.

(27) McDonell, A. C.; Hambley, T. W.; Snow, M. R.; Wedd, A. G. *Aust. J. Chem.* **1983**, *36*, 253–258. Nicholson, T.; Lombardi, P.; Zubieta, J. *Polyhedron* **1987**, *6*, 1577–1585.

(28) Clegg, W.; Boyde, S.; Garner, C. D. *Acta Crystallogr.* **1988**, *C44*, 172–174.

(29) Davison, A.; DeVries, N.; Dewan, J.; Jones, A. *Inorg. Chem.* **1986**, *120*, L15–L16.

(30) Sergienko, V. S.; Porai-Koshits, M. A. *Koord. Khim.* **1982**, *8*, 251–257.

Table 13. Comparison of Re(III/II) and Tc(III/II) Electrochemical Potentials in Analogous Thiolato Diphosphine and Diarsine Complexes[a]

complex	$E°'$ (M(III/II)), V DMPE	 DIARS	$E°'$(DMPE) − $E°'$(DIARS), mV
trans-$[Tc(SMe)_2D_2]^+$	−0.550	−0.465	−85
cis-$[Tc(SPh)_2D_2]^+$	−0.299	−0.322	+23
trans-$[Re(SPh)_2D_2]^+$	−0.554	−0.476	−78
cis-$[Re(SPh)_2D_2]^+$	−0.521	−0.543	+22

complex	$E°'$(M(III/II)), V Tc	 Re	$E°'$(Tc) − $E°'$(Re), mV
cis-$[M(SPh)_2(DMPE)_2]^+$	−0.299	−0.521	+222
cis-$[M(SPh)_2(DIARS)_2]^+$	−0.322	−0.543	+221

complex	$E°'$(M(III/II)), V *cis*	 *trans*	$E°'$(*cis*) − $E°'$(*trans*), mV
$[Re(SPh)_2(DMPE)_2]^+$	−0.521	−0.554	+33
$[Re(SPh)_2(DIARS)_2]^+$	−0.543	−0.476	−67

[a] All are reversible at room temperature, $E°'$ *vs* Ag/AgCl (3 M NaCl) in 0.5 M TEAP/DMF. $E°'$ values were extracted from refs 11, 12, and 19 and herein.

the DPPE complex is the easiest, and the DEPE complex the hardest, to reduce. This sequence is identical to that noted above for the increasing energy of the most intense S → Re CT bands in the visible spectra. Thus the most strongly oxidizing metal center (DEPE) exhibits the S (π) → M (t_{2g}) transition of the lowest energy. (ii) In *cis*-$[M^{III}(SPh)_2D_2]^+$ complexes, the DMPE complex is easier to reduce than the DIARS complex for both Tc and Re. This is a reversal of the trend noted just above for the *trans* complexes. It has been previously speculated[12] that perhaps the rigid backbone of DIARS inhibits effective π overlap in the *cis* geometry; this phenomenon would account for the difficulty in reducing the M–DIARS center. (iii) Technetium *cis*-$[M^{III}(SPh)_2D_2]^+$ complexes are ~220 mV easier to reduce than their rhenium analogs. This redox behavior is the source of the main chemical differences between analogous technetium and rhenium complexes and has been well documented.[31] (iv) For $[Re(SPh)_2D_2]^+$, the *cis* complex of DMPE is 33 mV easier to reduce to Re(II) than is the *trans*. However, this *cis* complex with DIARS is 67 mV harder to reduce than the *trans*, implying that the DIARS complex is less able to stabilize the additional negative charge. Again, this may be due to the rigid DIARS backbone limiting the Tc → As π-back-bonding in the *cis* configuration.

Summary. The complex $[Re(SEt)_2(DIARS)_2]^+$ is prepared solely as the *trans* isomer, while $[Re(SPh)_2(DIARS)_2]^+$ exhibits both *cis* and *trans* isomers. Previous studies have shown that $[Re(SR)_2(DEPE)_2]^+$ and $[Re(SR)_2(DPPE)_2]^+$ complexes are always *trans*. The driving force for isomer selection in these complexes is mainly steric. There is no substantive structural difference between Tc(III) and Re(III) complexes of the type $[M(SR)_2(D)_2]^+$, where D = diphosphine or diarsine. Tc(III)/Re(III)–S bond lengths are remarkable in their constancy at 2.28–2.30 Å, regardless of the R-group on the thiol. Likewise, the Tc(III)/Re(III)–As lengths are consistently 2.49 Å. Longer Re–S and Re–As lengths are found in Re(V) complexes, which implicates both the thiol and arsine donor atoms as π-back-bonders.

With regard to redox potentials, Tc(III) and Re(III) show parallel behavior, even though Tc(III) complexes are ~220 mV easier to reduce than the analogous Re(III) complexes. For *trans*-$[M(SR)_2(D)_2]^+$ complexes, that with DPPE is easier to reduce than that with DIARS, which in turn is easier to reduce than that with DMPE, which is still easier to reduce than that with DEPE. For *cis*-$[M(SR)_2(D)_2]^+$ complexes, that with DMPE is easier to reduce than that with DIARS, which is opposite to the *trans* series, and which may result from ineffective π-overlap of the rigid DIARS ligands in the *cis* configuration.

The additional redox control provided by DIARS in this $[M(SR)_2(D)_2]^+$ series of complexes has radiopharmaceutical significance. We have been searching for a judicious choice of ligands that would provide the exact redox potential needed to allow a neutral ^{99m}Tc complex to exist in the blood without *in vivo* reduction (e.g. $[Tc^{III}Cl_2(DMPE)_2]^+$ undergoes reduction to the Tc(II) complex[25]) but barely so. This neutral complex would then have the possibility of crossing the blood/brain barrier[32] and undergo 1-equiv oxidation within brain tissue, which is relatively more oxidizing than blood.[33] The resulting cationic $^{99m}Tc^{III}$ complex might then be trapped long enough to allow scintographic imaging.[32] The evaluation and assessment of the influence of DIARS on the M(III/II) redox potential in $[M^{III/II}(SR)_2(D)_2]^{+/0}$ complexes provides another step toward achieving this goal.

Acknowledgment. Financial support by the National Institute of Health grants Nos. HL-21276 and CA-42179 (E.D.) and by Mallinckrodt, Inc. (E.D.), is gratefully acknowledged. These studies are especially indebted to the actions of the University of Cincinnati RSO. The diffractometer used herein was purchased through an NSF equipment grant to Wayne State University.

Supplementary Material Available: Tables of supplementary crystallographic data, bond lengths, bond angles, thermal parameters, and hydrogen parameters for $[Re(SC_6H_5)_2(DIARS)_2](C_3H_5O_2)\cdot H_2O$ (Tables A–E), $[ReOCl(SC_6H_5)_2(DIARS)]$ (Tables F–J), and $[Re(SCH_2CH_3)_2(DIARS)_2]PF_6$ (Tables K–N) (18 pages). Ordering information is given on any current masthead page.

---

(31) Hurst, R. W.; Heineman, W. R.; Deutsch, E. *Inorg. Chem.* **1981**, *20*, 3298–3303.

(32) Neves, M.; Libson, K.; Deutsch, E. *Nucl. Med. Biol.* **1987**, *14*, 503–510.

(33) Bodor, N.; Prokai, L.; Wu, W.-M.; Farag, H.; Jonalagadda, S.; Kawamura, M.; Simpkins, J. *Science* **1992**, *257*, 1698–1700.